HOKKAIDO UNIVERSITY

Title	Orosomucoid 1 is involved in the development of chronic allograft rejection after kidney transplantation
Author(s)	Higuchi, Haruka; Kamimura, Daisuke; Jiang, Jing-Jing; Atsumi, Toru; Iwami, Daiki; Hotta, Kiyohiko; Harada, Hiroshi; Takada, Yusuke; Kanno-Okada, Hiromi; Hatanaka, Kanako C.; Tanaka, Yuki; Shinohara, Nobuo; Murakami, Masaaki
Citation	International immunology, 32(5), 335-346 https://doi.org/10.1093/intimm/dxaa003
Issue Date	2020-05
Doc URL	http://hdl.handle.net/2115/81115
Rights	This is a pre-copyedited, author-produced version of an article accepted for publication in International Immunology following peer review. The version of record Haruka Higuchi, Daisuke Kamimura, Jing-Jing Jiang, Toru Atsumi, Daiki Iwami, Kiyohiko Hotta, Hiroshi Harada, Yusuke Takada, Hiromi Kanno-Okada, Kanako C Hatanaka, Yuki Tanaka, Nobuo Shinohara, Masaaki Murakami, Orosomucoid 1 is involved in the development of chronic allograft rejection after kidney transplantation, International Immunology, Volume 32, Issue 5, May 2020, Pages 335-346, is available online at: https://doi.org/10.1093/intimm/dxaa003.
Type	article (author version)
Additional Information	There are other files related to this item in HUSCAP. Check the above URL.
File Information	Int Immunol_32_335.pdf

Instructions for use

Orosomucoid 1 is involved in the development of chronic allograft rejection after kidney transplantation.

Haruka Higuchi[1,2*], Daisuke Kamimura[1*], Jing-Jing Jiang[1*], Toru Atsumi[1], Daiki Iwami[2], Kiyohiko Hotta[2], Hiroshi Harada[4], Yusuke Takada[1,2], Hiromi Kanno-Okada[3], Kanako C. Hatanaka[3], Yuki Tanaka[1], Nobuo Shinohara[2], and Masaaki Murakami[1]

1, Division of Molecular Psychoimmunology, Institute for Genetic Medicine and Graduate School of Medicine, Hokkaido University, Sapporo 060-0815, Japan

2, Department of Renal and Genitourinary Surgery, Graduate School of Medicine, Hokkaido University, Sapporo 060-8638, Japan

3, Department of Surgical Pathology, Hokkaido University Hospital, Sapporo 060-8648, Japan

4, Department of Kidney Transplant Surgery, Sapporo City General Hospital, Sapporo 060-8604, Japan

*equal contribution

Running Title: Urinary ORM1 in chronic allograft rejection

Correspondence: Masaaki Murakami, North 15 West 7, Kita-ku, Sapporo, 060-0815 Japan, telephone: 81-11-706-5120, murakami@igm.hokudai.ac.jp and Nobuo Shinohara, North 15 West 7, Kita-ku, Sapporo, 060-8638 Japan,telephone: 81-11-706-5966, nozomis@mbj.nifty.com

Lead contact: Masaaki Murakami, murakami@igm.hokudai.ac.jp

Key Words: chronic kidney allograft rejection, kidney transplantation, chronic active antibody-mediated rejection, orosomucoid 1, inflammation amplifier, biomarker

Abbreviations : CAAMR, chronic active antibody-mediated rejection; CRP, C-reactive protein; CNI-T, calcineurin inhibitor toxicity; eGFR, estimated glomerular filtration rate; IFTA, interstitial fibrosis and tubular atrophy; HKF, human kidney fibroblasts; HRGEC, human renal glomerular microvascular endothelial cells; HRMC, human renal mesangial cells; KTR, kidney transplant recipients; NAG, N-acetyl-β-D-glucosaminidase; ORM1, orosomucoid 1; RPTEC, renal proximal tubule epithelial cells; Scr, serum creatinine

Abstract

Chronic allograft rejection is the most common cause of long-term allograft failure. One reason is that current diagnostics and therapeutics for chronic allograft rejection are very limited. We here show that enhanced NFκB signaling in kidney grafts contributes to chronic active antibody-mediated rejection (CAAMR), which is a major pathology of chronic kidney allograft rejections. Moreover, we found that urinary orosomucoid 1 (ORM1) is a candidate marker molecule and therapeutic target for CAAMR. Indeed, urinary ORM1 concentration was significantly higher in kidney transplant recipients pathologically diagnosed with CAAMR than in kidney transplant recipients with normal histology, calcineurin inhibitor toxicity, or interstitial fibrosis and tubular atrophy. Additionally, we found that kidney biopsy samples with CAAMR expressed more ORM1 and had higher NFκB and STAT3 activation in tubular cells than samples from non-CAAMR samples. Consistently, ORM1 production was induced after cytokine-mediated NFκB and STAT3 activation in primary kidney tubular cells. The loss- and gain-of-function of ORM1 suppressed and promoted NFκB activation, respectively. Finally, ORM1 enhanced NFκB-mediated inflammation development in vivo. These results suggest that an enhanced NFκB-dependent pathway following NFκB and STAT3 activation in the grafts is involved in the development of chronic allograft rejection after kidney transplantation and that ORM1 is a non-invasive candidate biomarker and possible therapeutic target for chronic kidney allograft rejection.

Introduction

Kidney transplantation is the most effective replacement therapy for end stage renal disease. Data from the U.S. Renal Data System (2013) (https://www.usrds.org/) indicate that survival after renal transplantation is significantly better than treatment with dialysis. Improved immunosuppressants have significantly reduced the risk of acute rejection, and short-term graft survival has similarly improved (1). However, chronic allograft rejection via slow, progressive diseases such as chronic active antibody-mediated rejection (CAAMR) has proven a more difficult problem (1,2). Further, pathological changes occur gradually even without clinical signs followed by dysregulation of the organ function. Allograft biopsies are considered the gold standard for the diagnosis of chronic allograft graft rejection (3), but the outcome after diagnosis, especially by episode biopsies, is still poor. A reliable clinical index to determine when a biopsy should be performed is therefore awaited. In addition to issues in diagnostic tests, the balance between immunosuppressive agents, opportunistic infection and other adverse effects is also a major problem in post-transplant treatment (4). Moreover, there is no effective agent for the treatment of chronic allograft graft rejection including CAAMR. Thus, sensitive, non-invasive molecular biomarkers and novel therapeutic molecular targets for chronic kidney allograft rejection are urgently needed.

Recent studies have suggested that chronic inflammation is critical for the development of various diseases. We have found a molecular mechanism for chronic inflammation originally called the IL-6 amplifier (now termed the inflammation amplifier) (5-7). The amplifier is activated by the concomitant activation of two transcription factors, NFκB and STAT3, in non-immune cells including synovial cells, fibroblasts, and endothelial cells (5-7). The co-activation of NFκB and STAT3 synergistically activates the NFκB signal to enhance the production of various pro-inflammatory factors, such as IL-6, chemokines and growth factors, and promotes chronic inflammation in the affected tissues. Inactivation of the inflammation amplifier significantly improves disease outcomes in mouse models of multiple sclerosis, dermatitis, uveoretinitis and rheumatoid arthritis (5,8-18). Further, its activation is critically involved in the development of a murine model of allogenic chronic rejection and is observed in human allogeneic lung transplantation with chronic rejection phenotypes (19,20). Genome-wide screenings have identified over 1,000 positive regulators and 500 target genes of the inflammation amplifier machinery in which human disease–associated genes including transplantation-related ones are highly enriched (10).

One of the genes identified by the genome wide-screenings was orosomucoid 1 (ORM1, also known

as α1-acid glycoprotein 1), an acute phase plasma protein known to increase during inflammation (21). Human liver cells are a major site of ORM1 production, but ORM1 can also be produced in endothelial cells and some tumor cells (22). ORM1 has been reported to function as a transport protein in the bloodstream (23,24). It is also known to activate NFκB, p38 and JNK pathways in macrophages, although this effect is weaker than LPS (25). The elevation of urinary ORM1 has been reported in several diseases such as chronic heart failure, rheumatoid arthritis and bladder cancer, possibly due to an increased permeability of glomerular endothelial cells (26-28). It is also recently shown that urinary ORM1 is increased in patients at the progressive chronic kidney disease stage of sickle cell anemia (29). However, the cellular sources and biological functions of renal ORM1, particularly during chronic kidney allograft rejection, are not fully understood.

In the current study, we found that activation of the inflammation amplifier in grafts is involved in the development of chronic allograft rejection after kidney transplantation and that ORM1 is both a target gene and a positive regulator of the inflammation amplifier in kidney tubular cells. Injections of ORM1 aggravated the inflammation amplifier in an arthritis mouse model. Finally, analyses of clinical specimens suggested that ORM1 produced from kidney tubular cells in response to inflammatory stimuli contributes to the high levels of urinary ORM1 detected in patients with CAAMR. These results strongly suggest that ORM1 is a candidate therapeutic target and a non-invasive diagnostic biomarker for chronic kidney allograft rejections.

Materials and Methods
Patients and controls
Serum and urine samples were collected from kidney transplant recipients (KTR) who underwent protocol allograft biopsies from November 2015 to January 2017 at Hokkaido University Hospital and Sapporo City General Hospital. All patients had a follow-up period of 3 months or longer after kidney transplantation. The following patients were excluded from the study: those with microscopic hematuria (more than 5 red blood cells per high power field), because ORM1 is detected in human blood at concentrations about 1,000 times higher than in urine; urinary tract infections; severe acute infection; and malignant disease. Clean-catch urine samples and blood samples from KTR were collected upon admission for protocol biopsy or upon outpatient visit for follow up. Each urine sample was centrifuged at 1,500 g for 5 min at 4℃. Blood samples were centrifuged at 3,000 g for 10 min at 4℃. Supernatants of the urine and blood samples were stored at -80℃ for further analysis. Clinical data such as serum creatinine (SCr), C-reactive protein (CRP), urinary protein, urinary albumin, urinary N-acetyl-β-D-glucosaminidase (NAG), and estimated glomerular filtration rate (eGFR) were collected. The use of these samples was approved by an ethics committee at Hokkaido University Hospital. All patients gave written informed consent to participate in the study protocol. The pathological diagnosis was conducted according to the Banff Classification 2013 (30) by experienced pathologists at Hokkaido University Hospital.

Cytokine-induced arthritis model mice
F759 mice were backcrossed with C57BL/6 mice for more than 10 generations. All mice were maintained under specific pathogen-free conditions according to the protocols of Hokkaido University. The protocols for animal experiments were approved by the Institutional Animal Care and Use Committees of Hokkaido University. The cytokine-induced arthritis model using F759 mice was reported previously (8,10,11,13,15-17,31). In this study, to examine the enhancing effect of ORM1, low doses (10 ng each) of IL-6 (Toray Industries, Tokyo, Japan) and IL-17 (PeproTech, Rocky Hill, NJ), which do not induce full-blown arthritis, were injected at the ankle joints of F759 mice with or without 10 μg purified α1 acid glycoprotein (Sigma Aldrich, St. Louis, MI) on days 0, 1 and 2. The severity of the arthritis was determined based on the rigidity of the ankle joints owing to inflammation. Averages for a single point in one leg ankle joint from each mouse were used for the clinical assessment (8,10,11,13,15-17,31).

Tracheal heterotopic transplantation model mice

139   C57BL/6 and C3H/He mice were obtained from SLC Japan and maintained under specific
140   pathogen-free conditions according to the protocols of Hokkaido University. The protocols for
141   animal experiments were approved by the Institutional Animal Care and Use Committees of
142   Hokkaido University. The transplantation method used was described previously (19,32,33). In brief,
143   the mice were euthanized, and the trachea were resected. The isolated trachea were incubated with
144   50 μM of control or mouse ORM1 siRNA (Accell non-targeting siRNA and Accell SMARTpool,
145   Dharmacon) mixed with an siRNA delivery reagent containing a viral envelope derived from the
146   hemagglutinating virus of Japan (Genome-ONE Neo, Ishihara Sangyo Kaisha, LTD., Japan) (34-36).
147   Next, C57BL/6 recipient mice were anesthetized, small horizontal incisions were made, and
148   subcutaneous pockets were formed by blunt dissection. The trachea graft was placed heterotopically
149   into the pocket, and the wound was closed with surgical sutures. The grafts were harvested on day
150   14 after transplantation for H-E staining and immunohistochemistry using anti-mouse CD4 antibody
151   (RM4-5, eBioscience, Tokyo, Japan). Immunohistochemistry of frozen sections was performed as
152   described previously (9,12,14,18).
153
154   **Cells and stimulation conditions**
155   Human primary kidney cells used in the experiments include renal proximal tubule epithelial cells
156   (RPTEC; CC-2553, Lonza, Switzerland), human renal glomerular microvascular endothelial cells
157   (HRGEC; ACBRI128, Cell Systems, Kirkland, WA), kidney fibroblasts (HKF; H-6016, Cell
158   Biologics, Chicago, IL), and human renal mesangial cells (HRMC; #4200, ScienCell, Carlsbad, CA).
159   The cells were plated in 96-well plates (1×10^4 cells/well) and stimulated with some combination of
160   human IL-6 (100 ng/ml; Toray Industries) plus human soluble IL-6Rα (100 ng/ml; PeproTech),
161   human IL-17A (50 ng/ml; PeproTech), recombinant human ORM1 (1,000 ng/ml; Prospecbio,
162   Rehovot, Israel), and human TNFα (50 ng/ml; PeproTech) for 3, 6 or 24 hours after serum starvation.
163   Soluble IL-6Rα was added, because non-immune cells normally express only IL-6
164   signal-transducing receptor subunit gp130. Recombinant ORM1 was inactivated by incubating at
165   100°C for 10 min. The cells were harvested, and total RNA was prepared for real-time PCR. For
166   mechanistic analysis, RPTEC were immortalized using SV40 large T antigen. Immortalized RPTEC
167   showed a similar response to primary RPTEC following cytokine stimulation (Supplementary Fig. 1).
168   Human hepatoma Hep3B cells were stimulated overnight with IL-6/IL-6Rα, IL-17 or their
169   combination.
170
171   **Real-time PCR**
172   The 7300 fast real-time PCR system (Applied Biosystems, Tokyo, Japan) and SYBR Green PCR
173   master mix (Kapa Biosystems, Woburn, MA) were used to quantify the levels of target and GAPDH
174   mRNA. Total RNA was prepared using an RNA extraction kit and DNase I (NIPPON GENE, Tokyo,
175   Japan). The PCR primer pairs used for real-time PCR are described in Supplementary Table I.
176   The conditions for real-time PCR were 40 cycles at 94°C for 15 s followed by 40 cycles at 60°C for
177   60 s. The relative mRNA expression levels were normalized to the levels of GAPDH mRNA
178   expression.
179
180   **ORM1 measurement**
181   ORM1 concentrations in human urine samples or the culture medium were determined using the
182   Human α1-Acid Glycoprotein ELISA kit (R&D Systems, Minneapolis, MN), and ORM1 urinary
183   levels were normalized to urine creatinine. ORM1 concentrations in human blood samples were
184   measured by immunonephelometry (LSI Medience Corporation, Sapporo, Japan).
185
186   **Human small interfering RNAs**
187   Small interfering RNAs (siRNAs) against ORM1 (Sigma-Aldrich) and non-target control (Sigma
188   Mission SIC-001s; Sigma-Aldrich) were transfected into human RPTEC plated in 96-well plates (1
189    $\times 10^4$ cells/well) using Lipofectamine RNAiMAX (Thermo Fisher Scientific, Kanagawa, Japan).
190   Cells were incubated for 24 hours, and after 2 hours of starvation, they were stimulated with human

191 IL-6 (100 ng/ml) plus human soluble IL-6Rα (100 ng/ml) and/or human IL-17A (50 ng/ml) for 3
192 hours. RT-PCR analysis of the respective target was performed.
193
194 **Confocal microscopy**
195 RPTEC were stimulated with some combination of IL-6 (100 ng/ml) plus human soluble IL-6Rα
196 (100 ng/ml), recombinant ORM1 (1,000 ng/ml), and TNFα (10 ng/ml) for 30 min. The stimulated
197 cells were fixed in Cytofix solution (Cytofix/Cytoperm kit, BD Biosciences, San Jose, CA) for 20
198 min, permeabilized with Perm/Wash solution (Cytofix/Cytoperm kit), and incubated with rabbit
199 anti-p65 (1:50) for 1 hour. After washing, the cells were incubated with anti-rabbit Alexa Fluor
200 546-conjugated secondary antibody (1:200) and Hoechst 33342 nuclear stain (1:10,000) for 1 hour.
201 Phospho-STAT3 staining was performed using rabbit anti-phospho-Stat3 (Tyr705) monocloncal
202 antibody (1:100, Cell Signaling Technology, Danvers, MA), anti-rabbit Alexa Fluor 488-conjugated
203 secondary Ab (1:1,000) and Hoechst 33342 nuclear stain (1:10,000), according to the protocol
204 provided by Cell Signaling Technology. Confocal microscopy was performed with the LSM5 Pascal
205 system (Carl Zeiss, Oberkochen, Germany). The percentage of cells with more p65 or
206 phosphor-STAT3 localized in the nucleus than the cytoplasm was counted.
207
208 **Immunohistochemistry**
209 Paraffin sections were prepared after formalin fixation. Immunohistochemistry of serial sections was
210 performed using rabbit anti-STAT3 pY705 (1:200, Cell Signaling Technology, Danvers, MA), rabbit
211 anti-phospho NFκB p65 Ser276 (1:400, Sigma Aldrich), rabbit anti-ORM1 prestige antibody
212 HPA046438 (1:500, Sigma Aldrich), or control IgG (Cell Signaling Technology). The rabbit IgG
213 Elite ABC kit and ImmPACT DAB (Vector Laboratories, Burlingame, CA) were used for signal
214 enhancement and visualization, respectively.
215
216 **Statistical analysis**
217 Student t test (two-tailed), one-way ANOVA, Kruskal-Wallis test, and the Bonferroni
218 multiple-comparison method were used to test for significant differences among three
219 groups. A p value <0.05 was considered significant.
220

221 **Results**
222 **ORM1 in urine increased in patients with CAAMR diagnosis**
223 Because the inflammation amplifier is associated with various inflammatory diseases and disease
224 models including lung allograft rejections (5,8-20), we hypothesized that the amplifier is also
225 associated with the development and maintenance of CAAMR, a major pathology of chronic kidney
226 allograft rejections, and that genes induced by the inflammation amplifier may be candidate
227 biomarkers and therapeutic targets for CAAMR after kidney transplantation. In this study, we
228 focused on ORM1, a target gene of the inflammation amplifier (10), and measured urinary ORM1
229 levels in KTR. Among KTR who underwent protocol biopsies, we divided the recipients into four
230 groups: normal histology (n = 17), interstitial fibrosis and tubular atrophy (IFTA) (n = 30),
231 calcineurin inhibitor toxicity (CNI-T) (n = 25), and CAAMR (n = 17), according to the Banff
232 Classification 2013 (30). We did not include an acute rejection group, because these patients are rare
233 due to the development of effective immunosuppressants (37-39). Patient characteristics are shown
234 in Table 1. At the time of transplantation, the donor age and the percentage of living donors were not
235 significantly different among groups. The post transplantation period was significantly shorter in
236 normal histology patients than the other groups. The percentage of ABO incompatibility was not
237 significantly different among groups. The estimated eGFR was significantly lower in the CAAMR
238 group than the normal histology group, implying renal damage due to rejection (Fig. 1A). Serum
239 ORM1 levels were not changed among the four groups (Fig. 1B). Preliminary experiments suggested
240 that the expression patterns of several acute phase proteins were similar to that of ORM1 (data not
241 shown), and the serum CRP levels were not significantly different among groups (Table 1). Urinary
242 NAG levels, which are an indicator of renal tubular injury (40), were not changed either. However,
243 the urinary ORM1 level normalized to the creatinine (Cre) level in KTR was significantly higher in
244 the CAAMR group (40,549.0 ± 8,093.6 ng/mg Cre) compared with the CNI-T (11,202 ± 2,562
245 ng/mg Cre), IFTA (9,558.3 ± 1,935.8 ng/mg Cre), and normal histology (4,283.3 ± 1,010.4 ng/mg
246 Cre) groups (Fig. 1D). Our study used clinical samples from protocol biopsies (not episode biopsies).
247 Graft biopsies were performed without clinical criteria. Such biopsies are performed at Hokkaido
248 University Hospital and other Japanese hospitals due to the small number of kidney donors. The
249 urinary ORM1 and post transplantation periods among all patients were not significantly correlated
250 (Supplementary Fig. 2), most likely due to the different magnitude of the immune response against
251 different alloantigens including MHC on each graft. We applied receiver operating characteristic
252 (ROC) curves to assess the potential utility of urinary ORM1 in diagnosing CAAMR (Fig. 1E). ROC
253 analysis provided an optimum cut-off value of 7,090.4 ng/mg Cre, which corresponds to 94.1%
254 sensitivity and 65.3% specificity. The area under the ROC curve (AUC) of urinary ORM1 for the
255 diagnosis of CAAMR was 0.867. Thus, urinary ORM1 increases in patients with CAAMR and
256 might be a sensitive, non-invasive candidate marker for chronic kidney rejection.
257
258 **Strong expression of ORM1 and activation of NFκB and STAT3 in tubule cells of CAAMR**
259 **kidney allografts**
260 We next examined which renal cells express ORM1 in CAAMR. Immunohistochemistry strongly
261 stained for ORM1 in the brush border of tubular cells in CAAMR allograft samples compared with
262 allograft samples from recipients with normal histology (Fig. 2A). Our previous study showed that
263 ORM1 is induced by the inflammation amplifier (10). Consistent with that study, activated
264 (phosphorylated) forms of NFκB p65 and STAT3 were both strongly stained in the tubular cells of
265 CAAMR allografts, but phosphorylated NFκB p65 was stained considerably less so in the
266 glomerular cells of the CAAMR allografts (Fig. 2B and C, red arrows). Consistent with urinary
267 ORM1 levels (Fig. 1D), ORM1 expression and the phosphorylation of NFκB p65 and STAT3 were
268 less pronounced in the IFTA and CNI-T groups (Fig. 2A, 2D and 2E). These results suggest a
269 correlation between ORM1 induction in tubular cells and activation of the inflammation amplifier in
270 CAAMR samples.
271
272 **Primary tubule cells express ORM1 after cytokine stimulation, which induces STAT3 and**
273 **NFκB activation**

274 We then obtained various human primary cells that constitute the kidney to examine ORM1
275 production. We stimulated RPTEC, HRM, HRGEC, and HKF with the STAT3 stimulator IL-6 and
276 the NFκB stimulators IL-17 and TNFα or some combination of for 24 hours and measured the
277 mRNA expression of ORM1. The ORM1 mRNA expression was largely restricted to RPTEC (Fig.
278 3), which is consistent with the expression of ORM1 in the tubular cells of CAAMR allografts seen
279 in Fig. 2A. Following stimulation with the combination of IL-6 and IL-17, the protein level of
280 ORM1 was detected in the culture supernatant of RPTEC (Supplementary Fig. 3). This synergistic
281 effect of IL-6 and IL-17 was not observed in hepatoma cells even though ORM1 protein was at a
282 much higher concentration (Supplementary Fig. 3). Additionally, the expressions of IL-6 and CCL2
283 were synergistically induced in RPTEC (Fig. 3), suggesting activation of the inflammation amplifier
284 (5,8-20). These results suggest that tubular cells are the primary source of ORM1 in kidney and
285 enhance inflammation by activating the inflammation amplifier after cytokine stimulation.
286
287 **ORM1 enhances NFκB activation in vivo and in vitro**
288 Our previous study showed that epiregulin is induced by the inflammation amplifier and also
289 enhances activation of the inflammation amplifier, forming a positive feedback loop (10). Based on
290 this finding and the results in Fig. 3A, in which ORM1 was induced in RPTEC, we tested whether
291 ORM1 creates a similar positive feedback. For these experiments, RPTEC were stimulated with
292 recombinant ORM1 and IL-6. ORM1 significantly enhanced the expression of IL-6 and CCL2
293 mRNA in the presence of IL-6, which mimics the low level of inflammation seen with chronic
294 rejections (16) (Fig. 4A and 4B). The effect of ORM1 was dose-dependent and abrogated by heat
295 treatment, confirming LPS contamination in the recombinant ORM1 preparation was not a cause
296 (Supplementary Fig. 4). Consistently, ORM1 knockdown by siRNA significantly suppressed IL-6
297 mRNA induction after IL-6 and IL-17 treatment (Fig. 4C and 4D).
298 We then examined the effect of ORM1 on the inflammation amplifier in vivo. Because there is no
299 good model for CAAMR, we employed an amplifier-dependent mouse model, cytokine-induced
300 arthritis, by injecting IL-6 and IL-17 at the ankle joints of F759 mice (8,10,11,13,15-17,31). In this
301 study, we used low doses of IL-6 and IL-17 to induce only mild arthritis to evaluate the effect of
302 ORM1. Indeed, adding ORM1 to the cytokine injections significantly enhanced the arthritis (Fig.
303 4E). Furthermore, knockdown of ORM1 in the trachea graft improved the graft rejection response,
304 including epithelial cell desquamation and CD4+ T cell accumulation, in an allogeneic tracheal
305 heterotopic transplantation model that is dependent on IL-6 and IL-17 (19,32) and behaves as a
306 chronic rejection model (33) (Supplementary Fig. 5). These results suggest that ORM1 enhances the
307 activation of NFκB in vivo and in vitro.
308
309 **ORM1 promotes NFκB signaling**
310 Finally, to investigate the mechanism of the ORM1 action, we investigated the localization of NFκB
311 p65 by confocal microscopy in RPTEC after stimulation with IL-6, ORM1, or a combination of.
312 TNFα is a potent NFκB activator and was used as a positive control of nuclear translocation. NFκB
313 p65 translocation from the cytoplasm to the nucleus was clearly observed by the combination
314 stimulation, and the percentage of cells with NFκB p65 localized in the nucleus was significantly
315 higher (17.7%) compared to single stimulation with IL-6 (1.05%) or ORM1 (2.5%) (Fig. 5). On the
316 other hand, ORM1 did not affect the nuclear localization of phosphorylated STAT3 (Supplementary
317 Fig. 6). These data indicate that ORM1 reinforces activation of the inflammation amplifier in
318 RPTEC by promoting the nuclear translocation of NFκB p65.

Discussion

In the current study, we investigated potential diagnostic markers and candidate therapeutic targets for chronic kidney allograft rejection. We show evidence that activation of the inflammation amplifier in the allografts contributes to chronic kidney allograft rejection at least partially via ORM1 production and that ORM1 levels in urine increases in patients with chronic kidney allograft rejection. Thus, we suggested that the amplifier-mediated ORM1 expression in kidney is a candidate non-invasive diagnostic marker and a candidate therapeutic target for patients with CAAMR.

Urinary ORM1 levels were significantly higher in KTR with CAAMR than without. Because ORM1 is normally detected in human blood at concentrations about 1,000 times higher (45-98 mg/dL in males) than in urine (Fig. 1B) and because we found that urinary ORM1 and total protein levels were correlated (Supplementary Fig. 7A), it is possible that urinary ORM1 was due to a high leaking rate of proteins from the blood. We question this hypothesis, however. Although urinary total protein levels were significantly higher in CAAMR patients (Table 1), 8 of 17 CAAMR patients who had a urinary protein level less than 0.5 g/g Cre (diagnostic threshold) still showed significantly higher urinary ORM1 levels (Supplementary Fig. 7B and 7C). These results indicate that ORM1 in urine is a candidate early predictive marker for CAAMR before the manifestation of overt proteinuria directly from the blood leaking. Nevertheless, occult hematouria and proteinurea sometimes occur due to the recurrence of the original kidney disease after the transplantation. Therefore, future studies with higher sample numbers and validation cohorts are needed to verify the potential of ORM1 as an early predictive marker for CAAMR.

We also investigated the ORM1 function in chronic kidney allograft rejections. We found that ORM1 is expressed from kidney tubular cells after cytokine stimulation and stimulates the NFκB pathway to induce inflammatory mediators such as IL-6 and chemokines in the presence of IL-6. We also showed that ORM1 enhances development of the inflammation pathology in vivo. The phosphorylation of NFκB and STAT3 in kidney biopsy specimens from patients with CAAMR was more evident in tubular cells (Fig. 2B and 2C). Consistent with the phosphorylation in tubular cells, ORM1 expression was clearly detected in tubular cells of the kidney biopsy specimens and primary RPTEC (Fig. 2A and Fig. 3A). To our knowledge, this is the first report to suggest the production of ORM1 in kidney cells. Furthermore, we found that ORM1 together with IL-6 promotes the nuclear translocation of NFκB p65 in RPTEC (Fig. 5). These effects may be mediated through ORM1 receptors such as CCR5, Siglec-5 and TLR4/CD14 (25,41,42). The detailed mechanism for how ORM1 enhances NFκB signaling in RPTEC is a matter of future study.

IL-6 is known to be an important inflammatory cytokine in various diseases and disorders (10, 19, 20). Indeed, KTR have been reported to show elevated serum and urinary IL-6 levels when allografts are undergoing rejection (43-45). In response, tocilizumab, a humanized monoclonal antibody against the IL-6 receptor has recently commanded considerable attention for the treatment of chronic kidney allograft rejections including CAAMR (46,47). Our findings on the inflammation amplifier could explain a molecular mechanism for the IL-6 elevation in KTR and the effectiveness of anti-IL-6 receptor blockade against CAAMR. Consistently, it is reported that ORM1 transgenic mice are more susceptible to dextran sodium sulfate-induced colitis and have increased levels of serum IL-6 (48). On the other hand, several reports have demonstrated that ORM1 has anti-inflammatory properties. For example, the injection of ORM1 to mice inhibits the lethal shock induced by TNFα or LPS in combination with galactosamine, but pretreatment of ORM1 is necessary for the protection (49). In addition, intraperitoneal injections of ORM1 decreased fibrotic and inflammatory responses including the upregulation of α-smooth muscle actin, TGF-β, and IL-6 in the kidney 7 days after unilateral ureteral obstruction in mice (50). However, the ORM1 treatment did not significantly suppress the fibrotic and inflammatory responses at an earlier time point (day 3) (50), suggesting an indirect action of ORM1 on fibrosis and inflammation in this experimental setting. It is currently unknown what causes these contrasting inflammatory effects by ORM1. They may depend on the pathological phase, cell type, and/or other factors including IL-6 family cytokines

372   other than IL-6 itself, which are relatively anti-inflammatory (46). Elucidation of the cause is
373   necessary for future drug discovery targeting ORM1.
374
375   In summary, our results suggest that activation of the inflammation amplifier in grafts is involved in
376   the development of chronic allograft rejection after kidney transplantations and that urinary ORM1,
377   which is produced by kidney tubular cells in response to inflammatory stimuli, is a candidate
378   sensitive, non-invasive marker for chronic kidney allograft rejection before clinical manifestation
379   including proteinuria. Our data also revealed that ORM1 regulates the inflammation amplifier
380   activation in kidney tubular cells, providing a possible therapeutic strategy for chronic kidney
381   allograft rejection by targeting ORM1.

Author contribution

H.H., D.K., and M.M. wrote the manuscript and planned and analyzed the experiments; J.-J.J. performed the si-RNA knockdown experiments and generated the immortalized RPTEC; D.K. performed the in vivo experiments; H.K.-O. and K.C.H performed the pathological diagnosis of the kidney biopsies; D.I, K.H., H.H., and Y.T. managed follow up of the recipients and collected samples from the patients; T.A. provided guidance for the imaging studies; N.S. and M.M provided guidance in the planning and analysis of the experiments; D.K. and Y.T. performed experiments for the revision; H.H. performed all experiments not otherwise noted. All authors edited and approved the manuscript.

403 **Figure legends**
404 **Figure 1. Urinary ORM1 is a candidate marker for CAAMR**
405 (A-D) Urine and serum samples were collected from KTR with normal histology (Normal),
406 interstitial fibrosis and tubular atrophy (IFTA), calcineurin inhibitor toxicity (CNI-T), or chronic
407 active antibody-mediated rejection (CAAMR). eGFR rates (A) and urinary NAG levels (C) were
408 obtained from clinical data. Serum ORM1 levels (B) were measured by immunonephelometry.
409 Urinary ORM1 levels (D) were measured by ELISA and corrected by urine creatine levels. Data
410 represent the mean ± SEM. Statistical analyses were done by using the Kruskal-Wallis test and
411 Bonferroni correction. $*p<0.05$. $**p<0.001$.
412 (E) A ROC curve of urinary ORM1 levels was made by a series of 64 urine samples. The optimum
413 cut off was 7,019.5 ng/mg Cre, and the area under the ROC curve (AUC) for the diagnosis of
414 CAAMR was 0.87.
415
416 **Figure 2. ORM1 is expressed in tubular cells in CAAMR kidney allograft**
417 (A) Kidney allograft biopsy samples diagnosed as normal histology (Normal), CAAMR, IFTA, or
418 CNI-T were stained with anti-ORM1 or control antibody.
419 (B-E) Immunohistochemistry of phosphorylated NFκB p65 (pp65) or phosphorylated STAT3
420 (pSTAT3) using renal biopsy samples clinically diagnosed as Normal (B), CAAMR (C), IFTA (D),
421 or CNI-T (E). Red arrows are examples of pp65 or pSTAT3 positive cells.
422 Bars, 50 μm.
423
424 **Figure 3. Activation of the inflammation amplifier in human primary kidney cells**
425 (A) Renal proximal tubule epithelial cells (RPTEC), human renal mesangial cells (HRMC),
426 renal glomerular microvascular endothelial cells (HRGEC), and human kidney fibroblasts (HKF)
427 were stimulated with IL-6, IL-17, TNFα, or some combination thereof. ORM1 mRNA expression
428 levels were measured by RT-PCR.
429 (B) RPTEC were stimulated with IL-6, IL-17, TNFα, or some combination thereof. IL-6 mRNA
430 expression levels were measured by RT-PCR.
431 IL-6 and CCL2 mRNA expression levels were normalized to GAPDH mRNA expression.
432 The data represent the mean + S.D. Statistical analyses were done by Student's t tests (two-tailed).
433 $*p<0.05$, $**p<0.01$, and $***p<0.001$.
434
435 **Figure 4. ORM1 is a positive regulator of the inflammation amplifier**
436 (A, B) RPTEC were stimulated with IL-6 (IL6), ORM1, IL-6 and ORM1 (IL6+ORM1), or TNFα.
437 After 3 hours of stimulation, the mRNA expressions of IL-6 (A) and CCL2 (B) were measured by
438 RT-PCR. The relative mRNA expression levels were normalized to GAPDH mRNA expression.
439 (C, D) ORM1 was knocked down using three different siRNAs (si1-Orm1 to si3-Orm1) in RPTEC,
440 which were stimulated with IL-6 and IL-17A. The mRNA expressions of ORM1 (C) and IL-6 (D)
441 were measured by RT-PCR.
442 (E) Low doses of IL-6 and IL-17, which induce only mild arthritis, were injected with or without
443 ORM1 (10 μg per ankle) at the ankle joints of F759 mice on days 0, 1 and 2. Clinical scores of
444 arthritis are shown. Data represent the mean + S.E.M.
445 Statistical analyses were done by Student t tests (two-tailed). $*p<0.05$, and $**p<0.01$.
446
447 **Figure 5. ORM1 promotes NFκB signaling**
448 (A) RPTEC were stimulated with IL-6 (IL6), ORM1, IL-6 and ORM1 (IL6+ORM1), or TNFα
449 (positive control). After 30 minutes of stimulation, the localization of NFκB p65 (red) was observed
450 by confocal microscopy. Hoechst 33342 (cyan) was used for nuclear counter staining.
451 (B) Percentage of cells with NFκB p65 localized in the nucleus is shown. Statistical analyses were
452 done using Fisher's exact test. $*p<0.05$, $**p<0.01$, and $***p<0.001$.
453
454 **Supplementary Table 1.**
455 Primers used in this study.
456

457 **Supplementary Figure 1. Activation of the inflammation amplifier in immortalized RPTEC.**
458 Immortalized RPTEC were stimulated with IL-6, IL-17, IL-6 and IL-17, TNFα, or IL-6 and TNFα
459 for 3 hours. The mRNA expressions of IL-6 (A) and CCL2 (B) were measured by RT-PCR. The
460 relative mRNA expression levels were normalized to GAPDH mRNA expression. Statistical analysis
461 was done by Student's t tests (two-tailed). *p<0.05, **p<0.01, ***p<0.001.
462
463 **Supplementary Figure 2. No significant correlation between urinary ORM1 levels and post**
464 **transplantation periods**
465 Correlation analysis of urinary ORM1 levels and post transplantation periods is shown (r2 = 0.0467).
466
467 **Supplementary Figure 3. Protein levels of ORM1 in the culture supernatant**
468 RPTEC (A) and Hep3B cells (B) were stimulated overnight with IL-6, IL-17, or IL-6 and IL-17.
469 ORM1 levels in the culture supernatant were measured by human ORM1 ELISA. The data represent
470 the mean + S.D. (*** p<0.001).
471
472 **Supplementary Figure 4. Dose-response and heat-inactivation of ORM1**
473 RPTEC were stimulated for 3 hours with IL-6 and various concentrations of recombinant ORM1 or
474 heat-inactivated ORM1 (Heat). The mRNA expressions of CCL2 (A) and IL-6 (B) were measured
475 by RT-PCR. The relative mRNA expression levels were normalized to GAPDH mRNA expression.
476 Data represent the mean + S.D. Statistical analysis was done by one-way ANOVA. **p<0.01; ns,
477 not significant.
478
479 **Supplementary Figure 5. Improvement of chronic rejection response by ORM1 knockdown in**
480 **a tracheal heterotopic transplantation model**
481 The trachea of C57BL/6 (B6) or C3H/He (C3H) mice were incubated with control siRNA or ORM1
482 siRNA, followed by heterotopic transplantation to B6 mice. These trachea grafts were examined 14
483 days later by H-E staining (A) or immunohistochemical staining of CD4 (B). Quantification of (B) is
484 shown in (C). Data represent the mean + S.E.M. Statistical analysis was done by one-way ANOVA.
485 **p<0.01.
486
487 **Supplementary Figure 6. ORM1 did not enhance the nuclear translocation of STAT3**
488 (A) RPTEC were stimulated with IL-6, ORM1, IL-6 and ORM1 (IL6+ORM1), or TNFα. After 30
489 minutes of stimulation, the localization of phosphorylated STAT3 (red) was observed by confocal
490 microscopy. Hoechst 33342 (cyan) was used for nuclear counter staining.
491 (B) Percentage of cells with phosphorylated STAT3 localized in the nucleus is shown. Statistical
492 analyses were done using one-way ANOVA. *** p<0.001; ns, not significant.
493
494 **Supplementary Figure 7. Higher urinary ORM1 levels in CAAMR patients who had urinary**
495 **total protein levels less than 0.5.**
496 (A) Correlation analysis of urinary ORM1 and total protein levels in all samples. KTR with normal
497 histology (Normal), interstitial fibrosis and tubular atrophy (IFTA), calcineurin inhibitor toxicity
498 (CNI-T), or chronic active antibody-mediated rejection (CAAMR).
499 (B) Urinary total protein levels less than 0.5 g/g Cre in KTR are shown.
500 (C) Urinary ORM1 levels in KTR who had urinary total protein levels less than 0.5 g/g Cre are
501 shown.
502 The mean ± SEM are shown. Statistical analysis was done by the Kruskal-Wallis test. **p<0.01; ns,
503 not significant.
504

References

505

506   1   Iwami, D., Hotta, K., Sasaki, H., Hirose, T., Higuchi, H., Takada, Y., and Shinohara, N. 2017.
507   Highly Immunogenic DQB1 Mismatch Eplets Are Associated With Development of
508   Chronic Active Antibody-Mediated Rejection: A First Report From Japan. *Transplant Proc*
509   49:84.
510   2   Hara, S. 2016. Current pathological perspectives on chronic rejection in renal allografts.
511   *Clin Exp Nephrol.*
512   3   Van Loon, E., Lerut, E., and Naesens, M. 2017. The time dependency of renal allograft
513   histology. *Transplant international : official journal of the European Society for Organ*
514   *Transplantation* 30:1081.
515   4   Lea-Henry, T. and Chacko, B. 2017. Management considerations in the failing renal
516   allograft. *Nephrology (Carlton).*
517   5   Ogura, H., Murakami, M., Okuyama, Y., Tsuruoka, M., Kitabayashi, C., Kanamoto, M.,
518   Nishihara, M., Iwakura, Y., and Hirano, T. 2008. Interleukin-17 Promotes Autoimmunity by
519   Triggering a Positive-Feedback Loop via Interleukin-6 Induction. *Immunity.* 29:628.
520   6   Atsumi, T., Singh, R., Sabharwal, L., Bando, H., Jie, M., Arima, Y., Yamada, M., Harada, M.,
521   Jiang, J. J., Hirano, T., Kamimura, D., Ogura, H., and Murakami, M. 2014. Inflammation
522   amplifier, a new paradigm in cancer biology. *Cancer Research* 74:8.
523   7   Nakagawa, I., Kamimura, D., Atsumi, T., Arima, Y., and Murakami, M. 2015. Role of
524   Inflammation Amplifier-Induced Growth Factor Expression in the Development of
525   Inflammatory Diseases. *Critical reviews in immunology* 35:365.
526   8   Murakami, M., Okuyama, Y., Ogura, H., Asano, S., Arima, Y., Tsuruoka, M., Harada, M.,
527   Kanamoto, M., Sawa, Y., Iwakura, Y., Takatsu, K., Kamimura, D., and Hirano, T. 2011.
528   Local microbleeding facilitates IL-6- and IL-17-dependent arthritis in the absence of tissue
529   antigen recognition by activated T cells. *J Exp Med* 208:103.
530   9   Arima, Y., Harada, M., Kamimura, D., Park, J. H., Kawano, F., Yull, F. E., Kawamoto, T.,
531   Iwakura, Y., Betz, U. A., Marquez, G., Blackwell, T. S., Ohira, Y., Hirano, T., and Murakami,
532   M. 2012. Regional neural activation defines a gateway for autoreactive T cells to cross the
533   blood-brain barrier. *Cell* 148:447.
534   10   Murakami, M., Harada, M., Kamimura, D., Ogura, H., Okuyama, Y., Kumai, N., Okuyama,
535   A., Singh, R., Jiang, J. J., Atsumi, T., Shiraya, S., Nakatsuji, Y., Kinoshita, M., Kohsaka, H.,
536   Nishida, M., Sakoda, S., Miyasaka, N., Yamauchi-Takihara, K., and Hirano, T. 2013.
537   Disease-association analysis of an inflammation-related feedback loop. *Cell reports* 3:946.
538   11   Harada, M., Kamimura, D., Arima, Y., Kohsaka, H., Nakatsuji, Y., Nishida, M., Atsumi, T.,
539   Meng, J., Bando, H., Singh, R., Sabharwal, L., Jiang, J. J., Kumai, N., Miyasaka, N., Sakoda,
540   S., Yamauchi-Takihara, K., Ogura, H., Hirano, T., and Murakami, M. 2015. Temporal
541   expression of growth factors triggered by epiregulin regulates inflammation development. *J*
542   *Immunol* 194:1039.
543   12   Arima, Y., Kamimura, D., Atsumi, T., Harada, M., Kawamoto, T., Nishikawa, N., Stofkova,
544   A., Ohki, T., Higuchi, K., Morimoto, Y., Wieghofer, P., Okada, Y., Mori, Y., Sakoda, S.,
545   Saika, S., Yoshioka, Y., Komuro, I., Yamashita, T., Hirano, T., Prinz, M., and Murakami, M.
546   2015. A pain-mediated neural signal induces relapse in murine autoimmune
547   encephalomyelitis, a multiple sclerosis model. *eLife* 4:e08733.
548   13   Meng, J., Jiang, J. J., Atsumi, T., Bando, H., Okuyama, Y., Sabharwal, L., Nakagawa, I.,
549   Higuchi, H., Ota, M., Okawara, M., Ishitani, R., Nureki, O., Higo, D., Arima, Y., Ogura, H.,
550   Kamimura, D., and Murakami, M. 2016. Breakpoint Cluster Region-Mediated Inflammation
551   Is Dependent on Casein Kinase II. *J Immunol* 197:3111.
552   14   Arima, Y., Ohki, T., Nishikawa, N., Higuchi, K., Ota, M., Tanaka, Y., Nio-Kobayashi, J.,
553   Elfeky, M., Sakai, R., Mori, Y., Kawamoto, T., Stofkova, A., Sakashita, Y., Morimoto, Y.,
554   Kuwatani, M., Iwanaga, T., Yoshioka, Y., Sakamoto, N., Yoshimura, A., Takiguchi, M.,
555   Sakoda, S., Prinz, M., Kamimura, D., and Murakami, M. 2017. Brain micro-inflammation at
556   specific vessels dysregulates organ-homeostasis via the activation of a new neural circuit.
557   *eLife* 6:e25517.
558   15   Okuyama, Y., Tanaka, Y., Jiang, J. J., Kamimura, D., Nakamura, A., Ota, M., Ohki, T., Higo,

559   D., Ogura, H., Ishii, N., Atsumi, T., and Murakami, M. 2018. Bmi1 Regulates IkappaBalpha
560   Degradation via Association with the SCF Complex. *J Immunol* 201:2264.

561   16   Tanaka, Y., Sabharwal, L., Ota, M., Nakagawa, I., Jiang, J. J., Arima, Y., Ogura, H., Okochi,
562   M., Ishii, M., Kamimura, D., and Murakami, M. 2018. Presenilin 1 Regulates NF-kappaB
563   Activation via Association with Breakpoint Cluster Region and Casein Kinase II. *J Immunol*
564   201:2256.

565   17   Fujita, M., Yamamoto, Y., Jiang, J. J., Atsumi, T., Tanaka, Y., Ohki, T., Murao, N.,
566   Funayama, E., Hayashi, T., Osawa, M., Maeda, T., Kamimura, D., and Murakami, M. 2019.
567   NEDD4 Is Involved in Inflammation Development during Keloid Formation. *The Journal of*
568   *investigative dermatology* 139:333.

569   18   Stofkova, A., Kamimura, D., Ohki, T., Ota, M., Arima, Y., and Murakami, M. 2019.
570   Photopic light-mediated down-regulation of local alpha1A-adrenergic signaling protects
571   blood-retina barrier in experimental autoimmune uveoretinitis. *Scientific reports* 9:2353.

572   19   Lee, J., Nakagiri, T., Oto, T., Harada, M., Morii, E., Shintani, Y., Inoue, M., Iwakura, Y.,
573   Miyoshi, S., Okumura, M., Hirano, T., and Murakami, M. 2012. IL-6 amplifier,
574   NF-kappaB-triggered positive feedback for IL-6 signaling, in grafts is involved in
575   allogeneic rejection responses. *J Immunol* 189:1928.

576   20   Lee, J., Nakagiri, T., Kamimura, D., Harada, M., Oto, T., Susaki, Y., Shintani, Y., Inoue, M.,
577   Miyoshi, S., Morii, E., Hirano, T., Murakami, M., and Okumura, M. 2013. IL-6 amplifier
578   activation in epithelial regions of bronchi after allogeneic lung transplantation. *Int Immunol*
579   25:319.

580   21   Luo, Z., Lei, H., Sun, Y., Liu, X., and Su, D. F. 2015. Orosomucoid, an acute response
581   protein with multiple modulating activities. *J Physiol Biochem* 71:329.

582   22   Sorensson, J., Matejka, G. L., Ohlson, M., and Haraldsson, B. 1999. Human endothelial
583   cells produce orosomucoid, an important component of the capillary barrier. *The American*
584   *journal of physiology* 276:H530.

585   23   Ito, S., Tsuda, A., Momotsu, T., Igarashi, K., Kasahara, S., Satoh, K., and Shibata, A. 1989.
586   Urinary orosomucoid excretion rate in patients with non-insulin-dependent diabetes mellitus.
587   *Acta Endocrinol (Copenh)* 120:584.

588   24   Christiansen, M. S., Hesse, D., Ekbom, P., Hesse, U., Damm, P., Hommel, E.,
589   Feldt-Rasmussen, B., and Mathiesen, E. 2010. Increased urinary orosomucoid excretion
590   predicts preeclampsia in pregnant women with pregestational type 1 diabetes. *Diabetes Res*
591   *Clin Pract* 89:16.

592   25   Komori, H., Watanabe, H., Shuto, T., Kodama, A., Maeda, H., Watanabe, K., Kai, H.,
593   Otagiri, M., and Maruyama, T. 2012. alpha(1)-Acid glycoprotein up-regulates CD163 via
594   TLR4/CD14 protein pathway: possible protection against hemolysis-induced oxidative
595   stress. *J Biol Chem* 287:30688.

596   26   Hou, L. N., Li, F., Zeng, Q. C., Su, L., Chen, P. A., Xu, Z. H., Zhu, D. J., Liu, C. H., and Xu,
597   D. L. 2014. Excretion of urinary orosomucoid 1 protein is elevated in patients with chronic
598   heart failure. *PLoS One* 9:e107550.

599   27   Li, F., Yu, Z., Chen, P., Lin, G., Li, T., Hou, L., Du, Y., and Tan, W. 2016. The increased
600   excretion of urinary orosomucoid 1 as a useful biomarker for bladder cancer. *Am J Cancer*
601   *Res* 6:331.

602   28   Kang, M. J., Park, Y. J., You, S., Yoo, S. A., Choi, S., Kim, D. H., Cho, C. S., Yi, E. C.,
603   Hwang, D., and Kim, W. U. 2014. Urinary proteome profile predictive of disease activity in
604   rheumatoid arthritis. *J Proteome Res* 13:5206.

605   29   Jerebtsova, M., Saraf, S. L., Soni, S., Afangbedji, N., Lin, X., Raslan, R., Gordeuk, V. R.,
606   and Nekhai, S. 2018. Urinary orosomucoid is associated with progressive chronic kidney
607   disease stage in patients with sickle cell anemia. *Am J Hematol* 93:E107.

608   30   Haas, M., Sis, B., Racusen, L. C., Solez, K., Glotz, D., Colvin, R. B., Castro, M. C., David,
609   D. S., David-Neto, E., Bagnasco, S. M., Cendales, L. C., Cornell, L. D., Demetris, A. J.,
610   Drachenberg, C. B., Farver, C. F., Farris, A. B., 3rd, Gibson, I. W., Kraus, E., Liapis, H.,
611   Loupy, A., Nickeleit, V., Randhawa, P., Rodriguez, E. R., Rush, D., Smith, R. N., Tan, C. D.,
612   Wallace, W. D., Mengel, M., and Banff meeting report writing, c. 2014. Banff 2013 meeting

613   report: inclusion of c4d-negative antibody-mediated rejection and antibody-associated
614   arterial lesions. *Am J Transplant* 14:272.

615 31   Atsumi, T., Suzuki, H., Jiang, J. J., Okuyama, Y., Nakagawa, I., Ota, M., Tanaka, Y., Ohki,
616   T., Katsunuma, K., Nakajima, K., Hasegawa, Y., Ohara, O., Ogura, H., Arima, Y., Kamimura,
617   D., and Murakami, M. 2017. Rbm10 regulates inflammation development via alternative
618   splicing of Dnmt3b. *Int Immunol* 29:581.

619 32   Lemaître, P. H., Vokaer, B., Charbonnier, L. M., Iwakura, Y., Estenne, M., Goldman, M.,
620   Leo, O., Remmelink, M., and Le Moine, A. 2013. IL-17A mediates early post-transplant
621   lesions after heterotopic trachea allotransplantation in Mice. *PLoS One* 8:e70236.

622 33   Jungraithmayr, W., Jang, J. H., Schrepfer, S., Inci, I., and Weder, W. 2013. Small animal
623   models of experimental obliterative bronchiolitis. *Am J Respir Cell Mol Biol* 48:675.

624 34   Watanabe, T., Asano, N., Fichtner-Feigl, S., Gorelick, P. L., Tsuji, Y., Matsumoto, Y., Chiba,
625   T., Fuss, I. J., Kitani, A., and Strober, W. 2010. NOD1 contributes to mouse host defense
626   against Helicobacter pylori via induction of type I IFN and activation of the ISGF3
627   signaling pathway. *J Clin Invest* 120:1645.

628 35   Kon, S., Ishibashi, K., Katoh, H., Kitamoto, S., Shirai, T., Tanaka, S., Kajita, M., Ishikawa,
629   S., Yamauchi, H., Yako, Y., Kamasaki, T., Matsumoto, T., Watanabe, H., Egami, R., Sasaki,
630   A., Nishikawa, A., Kameda, I., Maruyama, T., Narumi, R., Morita, T., Sasaki, Y., Enoki, R.,
631   Honma, S., Imamura, H., Oshima, M., Soga, T., Miyazaki, J. I., Duchen, M. R., Nam, J. M.,
632   Onodera, Y., Yoshioka, S., Kikuta, J., Ishii, M., Imajo, M., Nishida, E., Fujioka, Y., Ohba, Y.,
633   Sato, T., and Fujita, Y. 2017. Cell competition with normal epithelial cells promotes apical
634   extrusion of transformed cells through metabolic changes. *Nat Cell Biol* 19:530.

635 36   Mitsuishi, Y., Taguchi, K., Kawatani, Y., Shibata, T., Nukiwa, T., Aburatani, H., Yamamoto,
636   M., and Motohashi, H. 2012. Nrf2 redirects glucose and glutamine into anabolic pathways
637   in metabolic reprogramming. *Cancer Cell* 22:66.

638 37   Bamoulid, J., Staeck, O., Halleck, F., Durr, M., Paliege, A., Lachmann, N., Brakemeier, S.,
639   Liefeldt, L., and Budde, K. 2015. Advances in pharmacotherapy to treat kidney transplant
640   rejection. *Expert Opin Pharmacother* 16:1627.

641 38   Hardinger, K. L., Koch, M. J., Bohl, D. J., Storch, G. A., and Brennan, D. C. 2010. BK-virus
642   and the impact of pre-emptive immunosuppression reduction: 5-year results. *Am J*
643   *Transplant* 10:407.

644 39   Kahn, D., Botha, J. F., Pascoe, M. D., Pontin, A. R., Halkett, J., and Tandon, V. 2000.
645   Withdrawal of cyclosporine in renal transplant recipients with acute tubular necrosis
646   improves renal function. *Transplant international : official journal of the European Society*
647   *for Organ Transplantation* 13 Suppl 1:S82.

648 40   Bosomworth, M. P., Aparicio, S. R., and Hay, A. W. 1999. Urine
649   N-acetyl-beta-D-glucosaminidase--a marker of tubular damage? *Nephrol Dial Transplant*
650   14:620.

651 41   Gunnarsson, P., Levander, L., Pahlsson, P., and Grenegard, M. 2007. The acute-phase
652   protein alpha 1-acid glycoprotein (AGP) induces rises in cytosolic Ca2+ in neutrophil
653   granulocytes via sialic acid binding immunoglobulin-like lectins (siglecs). *FASEB J*
654   21:4059.

655 42   Lei, H., Sun, Y., Luo, Z., Yourek, G., Gui, H., Yang, Y., Su, D. F., and Liu, X. 2016.
656   Fatigue-induced Orosomucoid 1 Acts on C-C Chemokine Receptor Type 5 to Enhance
657   Muscle Endurance. *Scientific reports* 6:18839.

658 43   Van Oers, M. H., Van der Heyden, A. A., and Aarden, L. A. 1988. Interleukin 6 (IL-6) in
659   serum and urine of renal transplant recipients. *Clin Exp Immunol* 71:314.

660 44   Casiraghi, F., Ruggenenti, P., Noris, M., Locatelli, G., Perico, N., Perna, A., and Remuzzi, G.
661   1997. Sequential monitoring of urine-soluble interleukin 2 receptor and interleukin 6
662   predicts acute rejection of human renal allografts before clinical or laboratory signs of renal
663   dysfunction. *Transplantation* 63:1508.

664 45   Sonkar, G. K., Singh, S., Sonkar, S. K., Singh, U., and Singh, R. G. 2013. Evaluation of
665   serum interleukin 6 and tumour necrosis factor alpha levels, and their association with
666   various non-immunological parameters in renal transplant recipients. *Singapore Med J*

667   54:511.
668 46 Wu, G., Chai, N., Kim, I., Klein, A. S., and Jordan, S. C. 2013. Monoclonal
669   anti-interleukin-6 receptor antibody attenuates donor-specific antibody responses in a mouse
670   model of allosensitization. *Transpl Immunol* 28:138.
671 47 Choi, J., Aubert, O., Vo, A., Loupy, A., Haas, M., Puliyanda, D., Kim, I., Louie, S., Kang, A.,
672   Peng, A., Kahwaji, J., Reinsmoen, N., Toyoda, M., and Jordan, S. C. 2017. Assessment of
673   Tocilizumab (Anti-Interleukin-6 Receptor Monoclonal) as a Potential Treatment for Chronic
674   Antibody-Mediated Rejection and Transplant Glomerulopathy in HLA-Sensitized Renal
675   Allograft Recipients. *Am J Transplant* 17:2381.
676 48 Hochepied, T., Wullaert, A., Berger, F. G., Baumann, H., Brouckaert, P., Steidler, L., and
677   Libert, C. 2002. Overexpression of alpha(1)-acid glycoprotein in transgenic mice leads to
678   sensitisation to acute colitis. *Gut* 51:398.
679 49 Libert, C., Brouckaert, P., and Fiers, W. 1994. Protection by alpha 1-acid glycoprotein
680   against tumor necrosis factor-induced lethality. *J Exp Med* 180:1571.
681 50 Bi, J., Watanabe, H., Fujimura, R., Nishida, K., Nakamura, R., Oshiro, S., Imafuku, T.,
682   Komori, H., Miyahisa, M., Tanaka, M., Matsushita, K., and Maruyama, T. 2018. A
683   downstream molecule of 1,25-dihydroxyvitamin D3, alpha-1-acid glycoprotein, protects
684   against mouse model of renal fibrosis. *Scientific reports* 8:17329.
685

	CAAMR	IFTA	CNI toxicity	Normal	P value
Number of patients	17	30	25	17	n.s.
Gender (Male/Female)	10/7	16/14	12/13	12/5	n.s.
Age at transplant (year)	46.0 (3-62)	44.5 (2-67)	43 (14-68)	38 (2-68)	n.s.
Donor age (year)	52 (35-74)	52 (23-70)	56 (33-78)	57.5 (24-69)	n.s.
Post transplant period (year)	10.5 (3.5-16)	6.25 (0.5-20)	8.5 (0.25-25)	2 (0.25-10)	** N vs. CNI-T ** N vs. IFTA *** N vs. CAAMR
Kidney age (donor age + post transplantation period in years)	62.5 (46-79.5)	58 (35-78)	65 (42-85)	58.5 (27-72)	* N vs. CNI-T * IFTA vs. CNI-T
ABO incompatible (%)	1 (5.8%)	7 (23.3%)	8 (32%)	6 (35.2%)	n.s.
Living donor (%)	15 (88.2 %)	21 (70%)	21 (84%)	16 (94.1%)	n.s.
CRP (mg/dL)	0.02 (0.01-1.64)	0.03 (0.02-0.44)	0.03 (0.02-0.53)	0.03 (0.02-0.18)	n.s.
Serum Cre (mg/dL)	1.47 (0.87-2.85)	1.14 (0.49-3.45)	1.15 (0.78-2.62)	1.05 (0.53-1.73)	* CNI-T vs. CAAMR ** N vs. CAAMR
eGFR (ml/min)	41.4 (15.9-58.7)	50.3 (19.3-96.2)	47.9 (20.6-77.2)	50.7 (37.8-123)	* N vs. CAAMR
Urinary TP/Cre (g/gCre)	0.53 (0.001-5.9)	0.05 (0.005-2.0)	0.03 (0.008-1.58)	0.02 (0.007-0.42)	* CNI-T vs. CAAMR * IFTA vs. CAAMR * N vs. CAAMR

CAAMR： chronic active antibody-mediated rejection
CNI-T: calcineurin inhibitor toxicity
Cre: creatinine
CRP: C reactive protein
eGFR: estimated glomerular filtration rate
IFTA: interstitial fibrosis and tubular atrophy
N: normal
TP: total protein
* p<0.05, **p<0.01, n.s.: not significant (Statistical analysis were done by using ANOVA and Kruskal-Wallis)
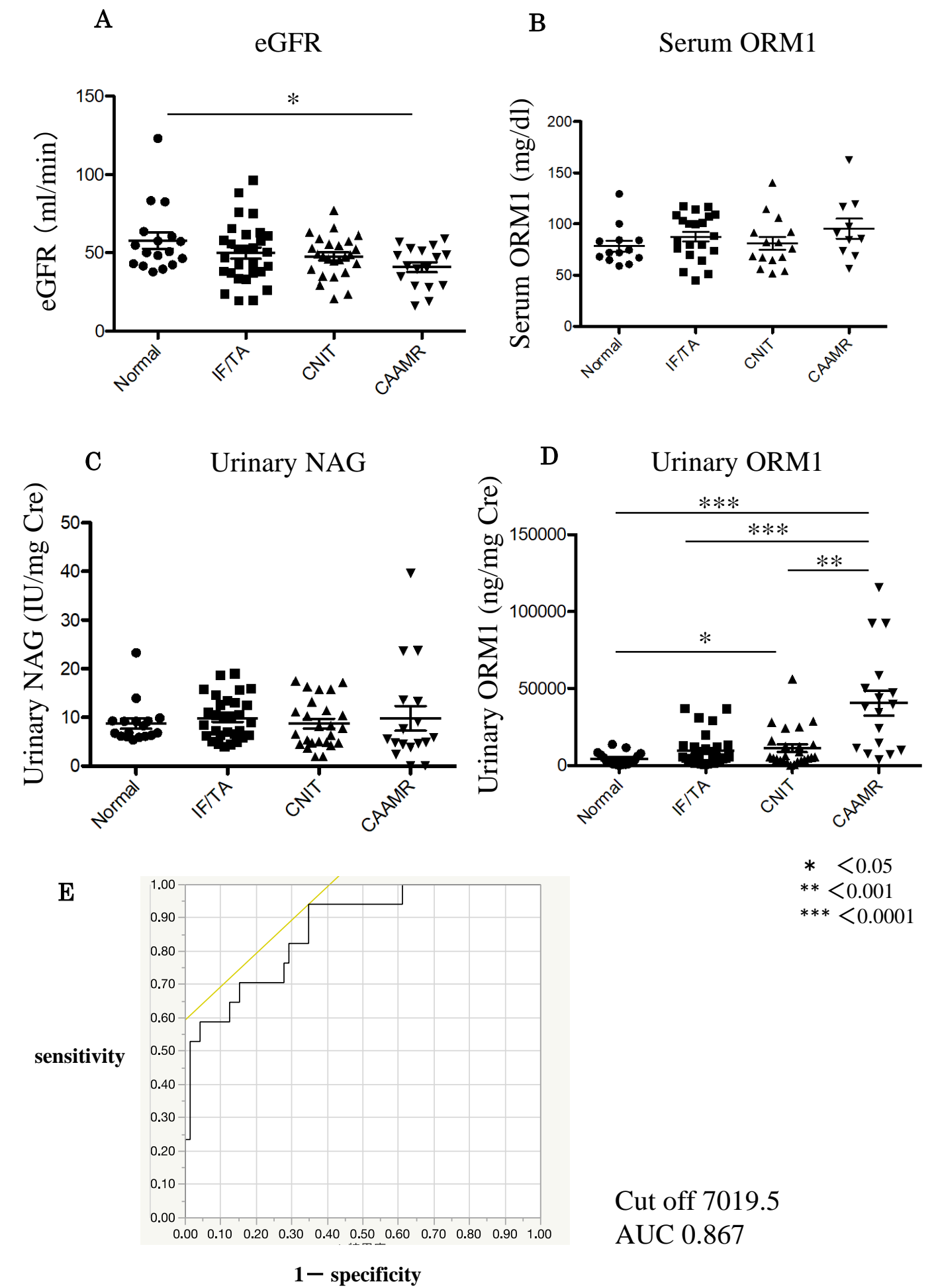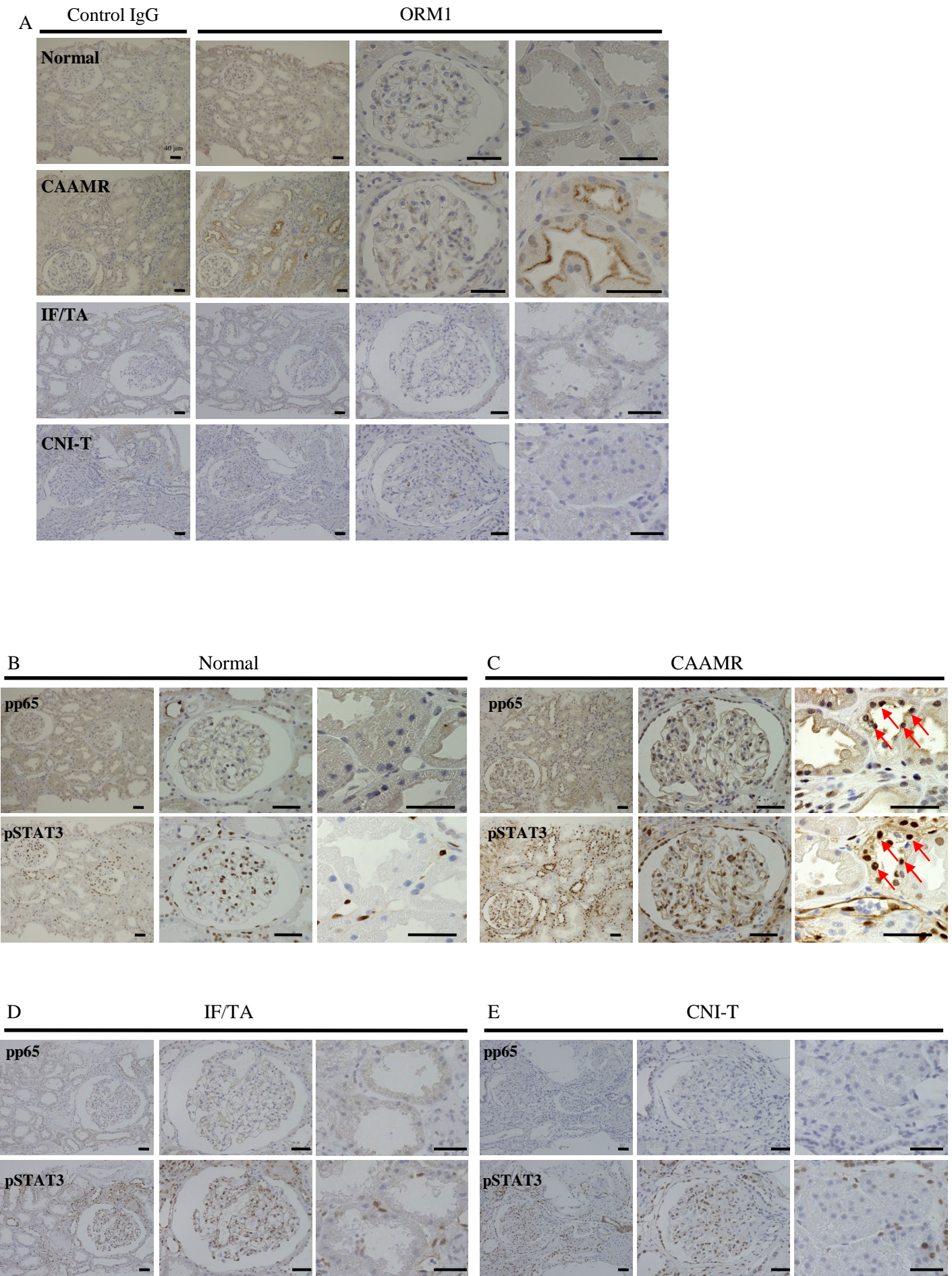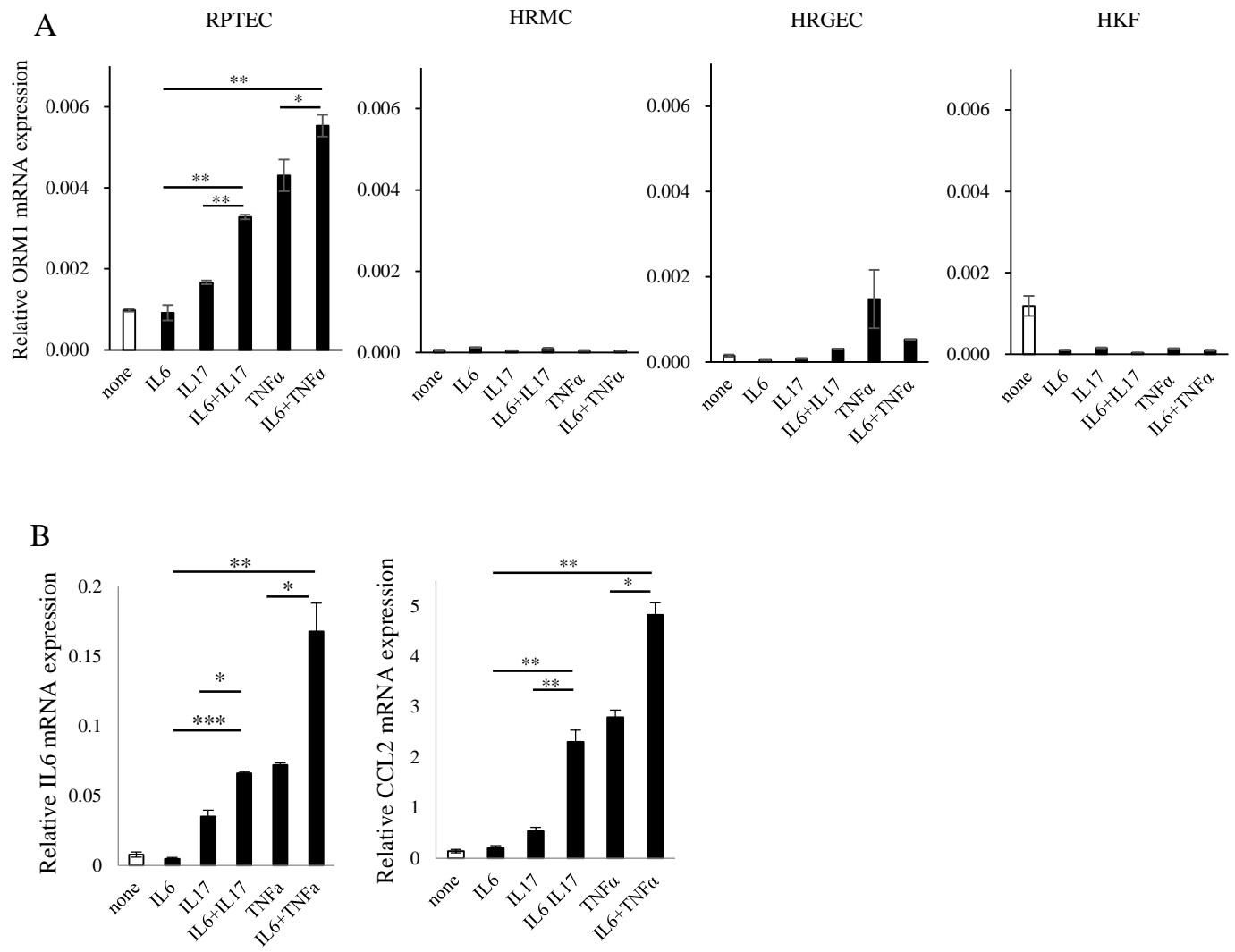
Figure 1

A

eGFR

B

Serum ORM1

C

Urinary NAG

D

Urinary ORM1

* < 0.05
** < 0.001
*** < 0.0001

E

sensitivity

1− specificity

Cut off 7019.5
AUC 0.867

Figure 2

Figure 3

A

RPTEC | HRMC | HRGEC | HKF

Relative ORM1 mRNA expression

Groups: none, IL6, IL17, IL6+IL17, TNFα, IL6+TNFα

B

Relative IL6 mRNA expression

Relative CCL2 mRNA expression

Groups: none, IL6, IL17, IL6+IL17, TNFα, IL6+TNFα

Figure 4

Figure 5

A

	none	IL6	ORM1	IL6+ORM1	TNFα
Hoechst					
p65					
Merge					

B

%